TRITON, PLUTO, CENTAURS, AND TRANS-NEPTUNIAN BODIES

DALE P. CRUIKSHANK
NASA Ames Research Center, Moffett Field, CA 94035-1000, USA

Received: 7 June 2004; Accepted in final form: 8 October 2004

Abstract. The diverse populations of icy bodies of the outer Solar System (OSS) give critical information on the composition and structure of the solar nebula and the early phases of planet formation. The two principal repositories of icy bodies are the Kuiper belt or disk, and the Oort Cloud, both of which are the source regions of the comets. Nearly 1000 individual Kuiper belt objects have been discovered; their dynamical distribution is a clue to the early outward migration and gravitational scattering power of Neptune. Pluto is perhaps the largest Kuiper belt object. Pluto is distinguished by its large satellite, a variable atmosphere, and a surface composed of several ices and probable organic solid materials that give it color. Triton is probably a former member of the Kuiper belt population, suggested by its retrograde orbit as a satellite of Neptune. Like Pluto, Triton has a variable atmosphere, compositionally diverse icy surface, and an organic atmospheric haze. Centaur objects appear to come from the Kuiper belt and occupy temporary orbits in the planetary zone; the compositional similarity of one well studied Centaur (5145 Pholus) to comets is notable. New discoveries continue apace, as observational surveys reveal new objects and refined observing techniques yield more physical information about specific bodies.

Keywords: Triton; Pluto; Centaurs; Kuiper Belt Objects; ice; infrared spectroscopy

1. Introduction

The sub-planet size bodies in the Solar System beyond Neptune, and including Neptune's large satellite Triton, are sometimes termed *ice dwarfs* because they are composed largely of solid H_2O and other frozen volatile materials. This term stands both in parallel and in contrast to *ice giants*, which characterizes Uranus and Neptune. Triton was found shortly after the discovery of Neptune itself, and because it is fairly bright it was thought from the outset to be relatively large in comparison to other planetary satellites. Pluto was discovered in 1930 as a result of a lengthy search for an external planet that was initiated to find the cause of a perceived gravitational perturbation to Neptune's orbit. It was later found that Neptune's motion was normal, and that Pluto was too small to have caused a noticeable effect in any case. Together with these bodies, we also consider the Centaurs because they formerly were trans-Neptunian objects, although they now have orbits within the planetary region.

The outer Solar System has long been thought to be the repository, and perhaps the place of origin, of the comets. Oort (1950) determined that the long-period ($P \geq 200$ y) and highly inclined comets are derived from a large reservoir of order

Space Science Reviews 116: 421–439, 2005.
DOI: 10.1007/s11214-005-1964-0

50,000 AU from the Sun, while Kuiper (1951) proposed that the comets with periods P≤200 y and lying near the ecliptic plane come from a disk-shaped reservoir that begins just beyond Neptune. Kuiper was led to this possibility by questioning the reality and meaning of an apparent edge to the mass distribution (with heliocentric distance) function of the Solar System that emerges when only the major planets are considered.

Oort's reservoir (the Oort Cloud) of small, icy bodies around the Sun cannot be detected directly, but is known from the slow leakage of individual objects that make their way to the inner Solar System and appear as comets. Similarly, Kuiper's reservoir went undetected, except for the short-period comets coming inward at the rate of a few tens of objects per year, until Jewitt and Luu (1993) discovered the first object beyond Pluto, 1992 QB1.

After some 50 years of study of the concepts proposed by Oort and Kuiper, it is recognized that both the Oort Cloud and the Kuiper belt tell important stories about the origin and evolution of the Solar System, and that similar structures may be common around other stars. With the discovery of nearly 1000 Kuiper belt objects (see below), the concept of a reservoir of short-period comets has advanced well beyond the abstract, and detailed studies of these objects in the aggregate and individually are in progress. This paper is a summary of current knowledge of the origins and physical properties of Triton, Pluto, the bodies in the Kuiper belt, and the Centaurs.

2. Triton

Among the objects discussed here, Triton is the only one for which we have direct knowledge from a close-up, although fleeting, view offered by a spacecraft. In August, 1989, the Voyager 2 spacecraft flew by Neptune, and 5 hours and 14 minutes later passed by Triton at a minimum distance of 39,800 km, conducting a battery of investigations of all aspects of these two bodies and their space environments (Stone and Miner, 1989; Cruikshank, 1995; Miner and Wessen, 2002). Only 40 percent of Triton was imaged, but an astonishing array of surface features was recorded, as well as surface deposits of dark material precipitating from erupting plumes and transported by winds driven by the sublimation of nitrogen from the sunlit south polar region. Three active plumes were seen ejecting material from the surface to a height of 8 km.

Triton's radius is 1352 km and its orbital period is 5.877 days. At a mean distance from Neptune of 14.3 R_N, it is in locked, synchronous rotation and its nearly circular orbit is retrograde. The mean density determined from Voyager observations is 2.06 g cm^{-3}.

Spectroscopy from ground-based telescopes shows the presence of absorption bands of solid N_2, CH_4 , CO_2, CO, and H_2O, all in the region 1.5-2.5 μm (Cruikshank *et al.*, 1998a; Quirico *et al.*, 1999). N_2 is found in the beta phase, which is

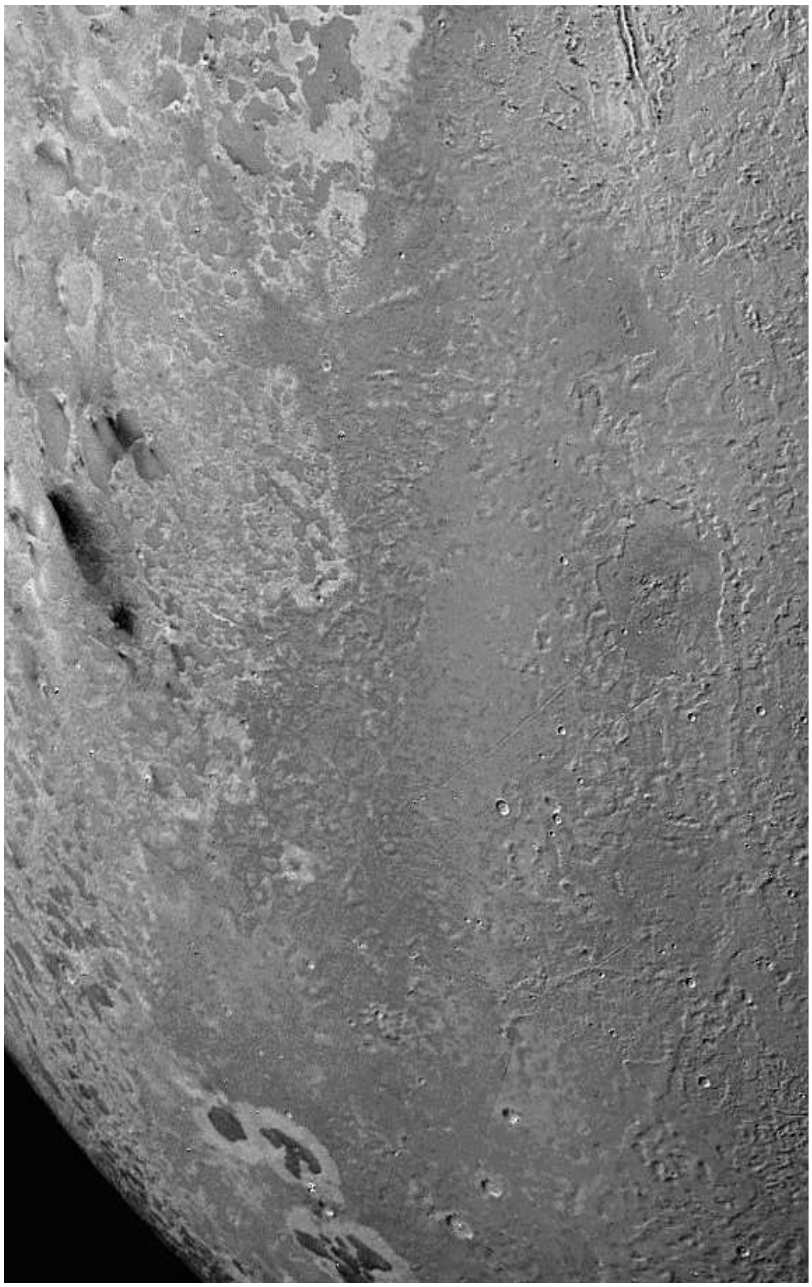

Figure 1. A section of Triton's surface (centered at ~38° E, -15° S). The direction to the S. pole is to the upper left. Left of center is a complex of dark spots (maculae) that appear to be surface deposits deposited by sublimation winds blowing from the S. pole. Right of center is a walled plain (Sipapu Planitia). At the bottom is a complex of flat, dark spots (maculae). At bottom center is the 27-km impact crater Mozamba, the largest seen on Triton. The boundary between the light colored S. polar material and the darker surface runs diagonally from top center toward the lower left side of the picture.

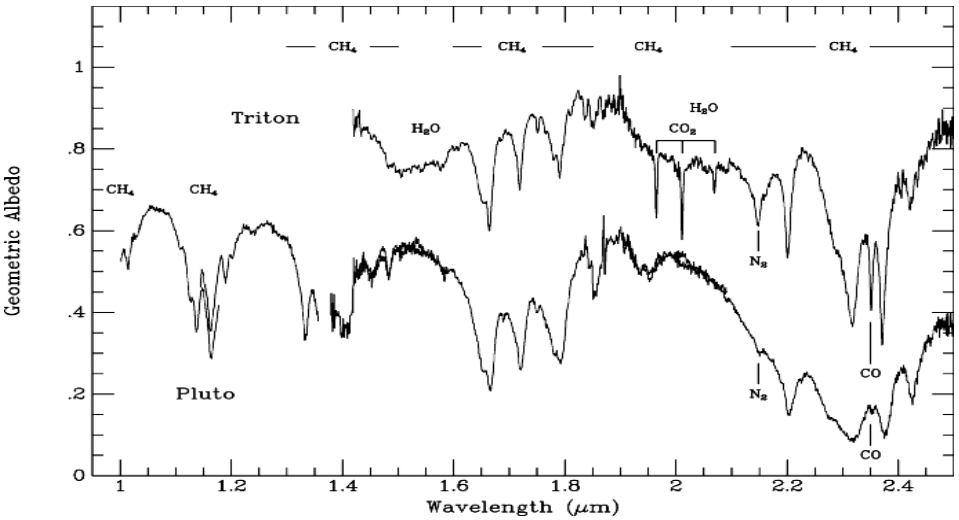

Figure 2. Reflectance spectra of Triton and Pluto from observations by T. C. Owen, D. P. Cruikshank, T. R. Geballe, C. de Bergh, and T. L. Roush with the UKIRT 3.8-m telescope. These and similar data from the same program serve as the basis for the analyses of Triton by Quirico *et al.* (1999) and of Pluto by Douté *et al.* (1999). The absorbing ice species that have been identified are indicated. H_2O has not been reliably identified on Pluto.

stable at $T \geq 36.8$ K. On Triton (and Pluto), solid N_2 occurs as large crystals with dimensions of order centimeters in which the optical pathlength is several centimeters. The CH_4 bands are shifted in wavelength (the matrix shift) by small amounts compared to pure CH_4 because the methane is dissolved in the N_2, appearing as an impurity in the large nitrogen crystals. In the 3-4 μm spectral region, Grundy *et al.* (2002) have found additional CH_4 ice absorption bands with additional unidentified absorption that may arise from nonvolatile solid surface components. Those nonvolatile components include the solid, low-albedo effluent from the plumes, as well as the material giving Triton's surface its overall coloration.

Changes in the color and spectral signature of Triton have been reported in data taken over the time interval 1977-2000 (e.g., Brown *et al.*, 1995). Such changes might arise with the condensation of new deposits of ices on the surface or from the sublimation of ice from large areas as a result of seasonal changes and/or geological activity.

The N_2 surface ice is the principal source of Triton's atmosphere, with the atmospheric pressure apparently in vapor pressure equilibrium at the prevailing temperature. The detection of an atmosphere with surface pressure $p = 16 \pm 3 \mu$bar by the Voyager radio science investigation (Tyler *et al.*, 1989; Yelle *et al.*, 1991) is consistent with the vapor pressure of N_2 at T$\sim$38 K (Broadfoot *et al.*, 1989). Triton's atmospheric gases have not yet been detected spectroscopically, but small amounts of CH_4 and CO are expected on the basis of their vapor pressures. CO_2 and

H_2O are not expected to contribute to the atmosphere because of their exceedingly low vapor pressures at the relevant temperature.

Evidence for change in Triton's surface temperature between the 1989 fly-by of Voyager 2 and 1997 comes from an increase in the pressure in the middle atmosphere ($z = 1400$ km) detected from observations of a stellar occultation (Elliot *et al.*, 1998). The pressure derived from the occultation is 2.3 ± 0.1 μbar, compared to the value of 0.8 ± 0.1 μbar extrapolated from the surface pressure measured by Voyager. The derived middle atmospheric temperature increased from 47 ± 1 K to 50.3 ± 0.5 K. Elliot *et al.* (1998) have calculated on the basis of the vapor pressure of the N_2 surface ice that the surface temperature increased from 37.5 K (in 1989) to 39.3 K in 1997. These changes could be caused by the migration of surface ices or frosts, changes in the optical properties of the surface frost (albedo, scattering efficiency, etc.), and changing heat input (from the Sun and from internal sources) to the ice. In this context, we note that Brown *et al.* (1995) reported a change in the strengths of the CH_4 bands in the spectrum of Triton in the interval 1980–1981. They suggested that a layer of obscuring material (e.g., N_2 frost) had been deposited on portions of Triton's surface in that time interval.

The atmosphere resulting from the sublimation of N_2, CH_4 , and CO ices from Triton's surface is photolyzed by Lyman-alpha photons from the Sun and the interstellar medium (Broadfoot *et al.*, 1989), producing the hydrocarbons C_2H_4, C_2H_6, and C_2H_2. These form haze particles and precipitate to the surface at rates calculated as 135, 28, and 1.3 g/cm^2/Gy, respectively (Krasnopolsky and Cruikshank, 1995). These hydrocarbons and other expected photolytic products (e.g., HCN) have not yet been detected in the spectrum of Triton (Quirico *et al.*, 1999); their concentrations are probably greatly diluted by the cycle of sublimation and condensation of the uppermost surface layers.

The large size of Triton and its circular, retrograde orbit impose special constraints on the origin of this satellite of Neptune. It is thought to have accreted in the region of the solar nebula beyond 30 AU as a member of the very large family of Kuiper belt objects, of which Triton and Pluto are perhaps the largest surviving members. Triton and Pluto share a very similar size and mean density ($\sim$2 g cm^{-3}), suggesting a bulk composition of about 60% silicate rocky material and 40% ice (McKinnon *et al.*, 1995).

In the early Solar System, in the final stages of its accretion, Neptune's orbit expanded, sweeping many Kuiper belt objects into its orbital resonances, thus dynamically stirring the population. Although Neptune's orbit now appears stable, its influence on the bodies in the inner Kuiper belt is still seen, as objects are perturbed both outward and inward to cross the orbits of the major planets. The latter such objects are called Centaurs, and their orbits are stable only for timescales of 10^6 to 10^7 y. Those objects scattered outward that remain in elliptical orbits are called scattered disk objects (see below).

In its late-accretion phase, Neptune's circumplanetary disk served both as a source region for the formation of satellites, and as a medium in which a passing

Kuiper belt object might be slowed sufficiently to permit gravitational capture. It is thought that Triton must have collided with a newly accreted satellite to dissipate enough energy to permit the capture. Subsequent circularization of the orbit resulted from the strong tidal interaction with Neptune as it made close approaches to the planet, at the same time completely disrupting, and perhaps accreting, such regular satellites that might have formed in the disk.

During the few hundred million years of orbital evolution, the dissipation of tidal energy produced a prodigious amount of heat in Triton, far more than needed to completely melt the body. The rate of heating depended on the rate of the evolution of the orbit, which in turn depended on the dissipative qualities of Triton's interior structure; liquid is highly dissipative, solid rock much less so. Thus, once an interior zone, such as a layer of ice, was melted, the heat became concentrated in that region, driving the volatile material toward the surface. Triton must have then had a very massive and vertically extended atmosphere, with temperatures in the range 100-200 K.

3. Pluto and Charon

The Pluto and Charon pair constitutes a binary system in a heliocentric orbit that is eccentric ($e = 0.246$) and inclined ($i = 17.14°$) to the ecliptic plane. Pluto's orbital period is in a 2:3 resonance with the orbital period of Neptune, and although Pluto's orbit crosses that of Neptune, the two planets cannot collide. Pluto was discovered photographically in 1930 in a search for a planet that was thought to perturb the orbit of Neptune, although it was later evident that Pluto is far too small to have such an effect. The satellite Charon was also found photographically, in 1978.

From observations with earth-based telescopes and orbiting observatories the basic physical properties of Pluto and Charon have been established. Their dimensions (Table I) and the orbital parameters of Charon were established through analysis of photometric observations of an extensive series of mutual transits and occultations that occurred in the interval 1985 – 1989 (Binzel and Hubbard, 1997). Fortuitously, these events occurred soon after the discovery of the satellite; if Charon had been discovered just ten years later, the mutual events would have been missed. From the dimensions of the bodies and the orbital parameters of Charon, the bulk densities of both objects have been determined (Table I); the density of Pluto is nearly identical to that of Triton, while Charon is about 15 percent less. At about the time the mutual events were concluding, high-resolution imaging with the Hubble Space Telescope and ground-based telescopes using adaptive optics systems gave the first optical images showing Charon separated from Pluto. Charon's orbital parameters have been refined using such high-definition images (Tholen and Buie, 1997).

Maps of Pluto's surface have been derived from observations of the mutual events (Young *et al.*, 2001) and from images with the Hubble Space Telescope

TABLE I
Physical Properties of Large Objects in the Outer Solar System

Object	Type	Radius (km)	Rotation period (days)	Mean density (g/cm^3)	Surface composition (molecular ices)	Notes
Triton	Neptune's satellite	1352	5.877	2.06	N_2,CH_4, CO, CO_2,H_2O	CH_4 dissolved in N_2 ice
Pluto	Planet	1150*	6.4	2.0±0.06	N_2,CH_4, CO, $(H_2O)^\dagger$	Some CH_4 dissolved in N_2, some pure. Locked synchronous rotation with Charon
Charon	Pluto's satellite	600-650	6.4	1.7±0.15	H_2O, NH_3 ‡	Locked synchronous rotation with Pluto
2003 VB_{12} Sedna	Anomalous	650-900	>20			Elliptical orbit perihelion 76 AU, aphelion 960 AU
50000 Quaoar	KBO	625				
20000 Varuna	KBO	450				
2004 DW	KBO	~800				
5145 Pholus	Centaur	~100	0.42		Organic solids, H_2O,CH_3OH, minerals	One of the reddest surfaces known
2060 Chiron	Centaur	~90	0.25		H_2O, low-albedo material	Episodic cometary activity
Phoebe	Saturn's Satellite	110	0.39		H_2O, CO_2 other?	Cassini results

* See text for notes on Pluto's radius
† Expected but not detected with certainty
‡ Possibly NH_4OH or some other hydrate of ammonia

(Stern *et al.*, 1997). These images show an uneven distribution of surface units of relatively low albedo on a brighter background, but are insufficient to define basins, craters, or other geological structures. On a large spatial scale, the albedo contrast on Pluto is more pronounced than that for any other solid Solar System body except Saturn's satellite Iapetus. The globally averaged color (0.3-1 μm) and albedo of Pluto can be satisfactorily modeled with a combination of spectrally neutral ices and a small quantity of tholin (Cruikshank *et al.*, 2005). The presence of this complex organic solid material is consistent with the composition of the surface ices and the atmosphere of Pluto, as noted below.

The composition of the surface of Pluto is similar in several respects to that of Triton, with a complex combination of the ices of N_2, CH_4, and CO (Owen *et al.*, 1993; Douté *et al.*, 1999). Methane is present in both a pure form and also dissolved in the solid N_2; the two forms can be distinguished spectroscopically by a small shift in the central wavelengths of the CH_4 bands that occurs when the molecules are incorporated in a matrix as a very dilute component. On Triton, the CH_4 is primarily dissolved in N_2 and a pure component has not been identified. In further contrast with Triton, CO_2 has not been clearly detected on Pluto, and the presence of H_2O ice in the spectrum is ambiguous (Grundy *et al.*, 2002). As with Triton, other condensed hydrocarbons and HCN are expected from photochemical reactions in the N_2 + CH_4 atmosphere (Krasnopolsky and Cruikshank, 1999) but have not yet been reliably detected.

The atmosphere of Pluto expected from the presence of volatile surface ices has been detected by stellar occultations (Elliot *et al.*, 1989), and is also a factor in the interpretation of the mutual transits and occultations with Charon. Methane gas, which is expected to be present in the atmosphere with a partial pressure $\sim 10^{-6}$ relative to N_2 has been weakly detected spectroscopically (Young *et al.*, 1997). A tentative detection at radio wavelengths of the J(2-1) CO line in Pluto's atmosphere has been reported by Bockelée-Morvan *et al.* (2001). Nitrogen, the principal atmospheric component expected on the basis of vapor pressure considerations, remains to be detected in the ultraviolet. The vapor pressure of N_2 is a strong function of temperature, ranging from 1.2 μbar at $T = 34$ K to 590 μbar at $T = 45$ K (Owen *et al.*, 1993). Pluto's surface is not isothermal; measurements with the ISO spacecraft suggest maximum dayside temperatures in the range 54-63 K (Lellouch *et al.*, 2000) and a porous upper few cm of the surface. The atmospheric surface pressure expected from the relatively high temperatures determined from the ISO data is somewhat higher than that inferred from stellar occultations.

The stellar occultation lightcurves, especially at minimum light, can be modeled with either an atmospheric haze (Elliot and Young, 1992) or with a thermal inversion layer in the lower stratosphere that optically masks a troposphere of unknown thickness (Stansberry *et al.*, 1994; Strobel *et al.*, 1996). In fact, a derivation of the exact diameter of Pluto depends upon the correct interpretation of the optical properties of the lower atmosphere. The exact diameter, in turn, is an important factor in establishing Pluto's mean density, the mass being well determined from

the motion of Charon. The Stansberry *et al.* (1994) model suggests a radius of 1190 km, although the unseen troposphere may be some 40 km deep, implying a radius of 1158 km.

The atmosphere of Pluto is variable on a time-scale of years. Observations of a recent (2002) stellar occultation (Elliot *et al.*, 2003; Sicardy *et al.*, 2003) probed Pluto's atmosphere, with the result that the shape of the occultation lightcurve was significantly different from that seen in a stellar occultation in 1988. The difference has been interpreted as an increase by a factor of about two in Pluto's atmospheric pressure; such a difference could arise from the warming of the N_2 surface ice by about 1 K.

Pluto's atmosphere is in a state of rapid hydrodynamic escape, in which light gases escaping by their thermal energy drag along heavier gases. Although this process is not seen on any other planet today, it may have been responsible for the rapid loss of hydrogen from the early atmosphere of the Earth and other terrestrial planets.

The reflectance spectrum of Charon shows the presence of H_2O ice (Dumas *et al.*, 2001) and an additional component that has an absorption band near 2.2 μm for which a hydrate of ammonia has been proposed (Brown and Calvin, 2000). No CH_4 is seen in Charon's spectrum, despite its prominence in the spectrum of Pluto. The H_2O band structure at 1.65 μm in Charon's spectrum indicates that the ice is crystalline, rather than amorphous. Overall, the albedo of Charon is lower than that of Pluto, it is more nearly spectrally neutral than Pluto, and it does not show a large variation in brightness with rotation.

The Pluto-Charon pair is presumed to have originated as a large member of the Kuiper belt (see below).

The *in situ* investigation of the Pluto-Charon pair is a primary science goal of NASA's New Horizons mission, currently intended for launch in 2006. The spacecraft will fly past Pluto and Charon approximately 10 years after launch, and then continue into the Kuiper belt region with the intent to fly by two or more KBOs. A large suite of imaging and spectroscopic investigations will be augmented by radio wavelength measurements of the atmosphere(s) of both bodies by the occultation technique used so successfully in many planetary flyby observations.

4. Centaurs and Trans-Neptunian Bodies

4.1. CENTAURS

Centaur objects are small bodies in heliocentric orbits that typically cross the orbits of one or more major planets. Their dynamical lifetimes are of order 10^6 - 10^7 y, and they are presumed to be derived from the Kuiper belt (see below). Some of them (e.g., 2060 Chiron, and P/Schwassmann-Wachmann 1) show episodic cometary activity. By mid-2004, $\sim$60 Centaur objects of various sizes were identified, but

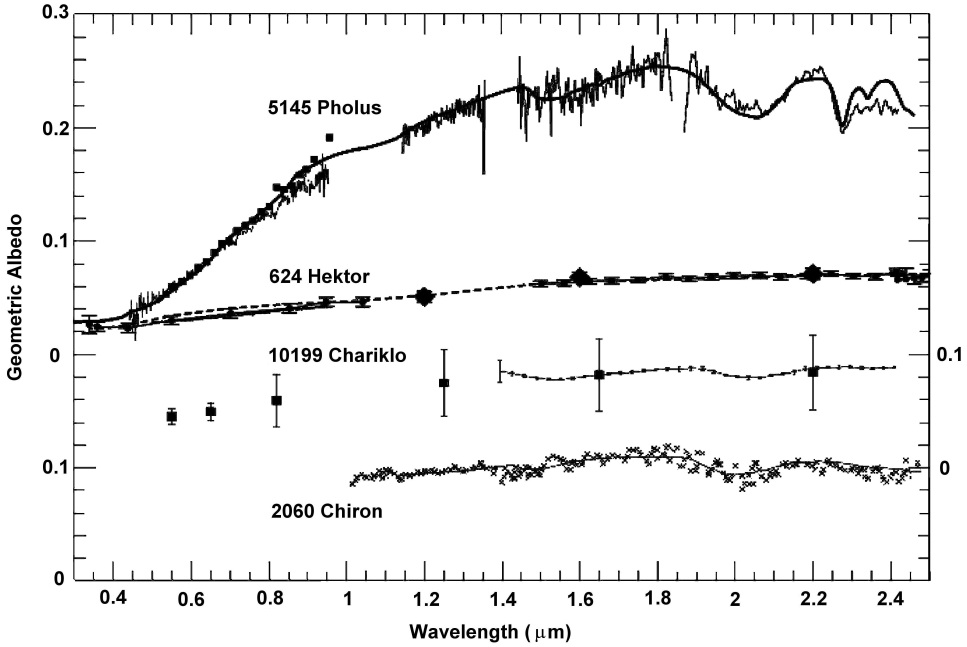

Figure 3. Reflectance spectra of the Centaurs 5145 Pholus, 10199 Chariklo, and 2060 Chiron, as well as the D-type Trojan asteroid 624 Hektor. The solid lines for Pholus and Chiron are models computed with scattering theory and the complex refractive indices of the components identified on each object. All three Centaurs show H_2O ice absorption bands at 1.5 and 2.0 μm, while Pholus shows additional absorption attributed to solid CH_3OH, olivine, and tholin. The spectrum of Hektor, while red in color, is otherwise featureless; the dashed line is a model computed with the mineral pyroxene as the main component.

the statistically projected number is of order 3000 (larger than 100 km diameter). Insofar as the Centaurs are dimensionally and compositionally representative of the Kuiper disk population, their physical properties are of interest, and because they are closer to the Earth, they are more easily observed than the distant and faint Kuiper belt objects. A detailed discussion of Centaur physical properties is given by Barucci *et al.* (2004).

Reflectance spectroscopy (0.4-2.4 μm) of many minerals and ices relevant to the surface compositions of Solar System objects show diagnostic absorption bands (e.g., Gaffey *et al.*, 1993; Brown and Cruikshank, 1993) that can be found in the spectra of asteroids, planetary satellites, and some KBOs and Centaurs. In addition, there is growing recognition of the importance of solid organic macromolecular material as a component of the surfaces of outer Solar System bodies, and the effect on the color and albedo that this material imparts (e.g., Andronico *et al.*, 1987; Hartmann *et al.*, 1987; Cruikshank, 1987; Luu *et al.*, 1994; Cruikshank and Dalle Ore, 2003). Here we show spectra of three Centaurs (Figure 3) that have varying degrees of diagnostic spectral activity.

2060 Chiron has a neutral reflectance at an albedo level of about 0.10, with weak but recognizable H_2O ice bands, notably at 2.0 μm. It shows intermittent cometary behavior in the form of variable brightness of what may be a permanent dust coma, even at its large heliocentric distance (8.45 AU at perihelion) (e.g., Hartmann *et al.*, 1990).

10199 Chariklo has a moderately red reflectance in the photovisual region and is nearly flat in reflectance in the near-infrared (Davies *et al.*, 1993). The photometric points in the near-infrared do not betray the presence of the weak bands of H_2O ice that are clearly seen in the spectrum by Brown *et al.* (1998). They modeled the spectrum 10199 Chariklo with an intimate mixture of H_2O ice, and a red material for which the complex indices were constructed. This computationally derived red component represents a natural material that is analogous to the complex refractory organic solids known as tholins.

5145 Pholus is exceptionally red among the Centaurs and the other small bodies of the outer Solar System observed to date (but see the discussion of Sedna below). The spectrum of 5145 Pholus has been recorded from 0.45 to 2.45 μm (Cruikshank *et al.*, 1998b, and sources quoted therein), as reproduced in Figure 3. The spectrum shows not only the strong red color at short wavelengths, but evidence for the 1.5 and 2.0 μm H_2O ice bands and an absorption complex at 2.27 μm.

The model of Pholus derived by Cruikshank *et al.* (1998b) and shown as the continuous solid line in Figure 3 consists of four spectrally active components, plus grains of amorphous carbon, which is spectrally neutral. Titan tholin (Khare *et al.*, 1984) imparts the steep reflectance between 0.45 and 1.0 μm, H_2O ice is responsible for the broad absorption bands a 1.5 and 2.0 μm, and CH_3OH ice appears to account for the band at 2.27 μm (but see Cruikshank *et al.*, 1998b, for details of this region). An additional component required to bring the model into accord with the data between 1.0-1.4 μm is olivine. This model incorporates the four most abundant materials known to occur in typical comet nuclei: organic solids, the silicate mineral olivine, water ice, and methanol ice, and while the relative abundances and details of the particle sizes and scattering parameters are model-dependent (Poulet *et al.*, 2002), the compositional similarity between this Centaur and comets is notable (Cruikshank *et al.*, 1998c).

4.2. TRANS-NEPTUNIAN BODIES

Since the pivotal discovery of 1992 QB_1 by Jewitt and Luu (1993), nearly 1000 objects with dimensions 50-600 km have been detected in the trans-Neptunian region. The largest of the bodies detected as of mid-2004 are listed in Table I.

Three distinct dynamical populations have become apparent as the discoveries continue. The first grouping, which includes the majority of the objects discovered to date, is known as the classical Kuiper belt. It consists of objects in near circular orbits with semi-major axes around 45 AU. These orbits are stable against Neptune's perturbations over the age of the Solar System. The second population

consists of objects in orbits with 2 : 3 resonance with Neptune, as in the case of Pluto. These objects are informally called "Plutinos"; the term is etymologically grotesque (an Italian-style diminutive of an anglicized classical Greek proper name), but it has gained widespread usage. Taken together, these two populations are frequently referred to as Kuiper belt objects (KBOs), a term that is used in this paper. The third population consists of objects in highly eccentric orbits with perihelia generally within the classical Kuiper belt (although some are inside Neptune's orbit), but with aphelia far outside. These bodies have been dynamically excited by Neptune; they are called scattered disk objects.

Direct imaging of a number of KBOs has shown that at least 5% of them are binary systems (Noll, 2004); the number of known binaries as of mid-2004 is 14. The angular separations of the two components of a binary are typically 0.25 - 0.5 arcsec. The relative dimensions of the two components vary widely from system to system, and are calculated from their relative brightness and estimates of their surface albedos. In general, the sizes of the two components tend to be very similar, and the barycenter of each of the systems is well outside the body of the primary.

Binary systems may have originated by collision and capture in the presence of a third body at a time when the Kuiper belt was at least 100 times more densely populated that it is now (Weidenschilling, 2002). Other dynamical scenarios have been proposed by Goldreich *et al.* (2002) and Funato *et al.* (2004). The statistical distribution of orbital eccentricities in a large sample of well observed binary KBOs may distinguish among the proposed origin scenarios. Collisions and close encounters among KBOs can disrupt some of the more widely separated and weakly bound binaries, and as noted by Noll (2004) the present population is probably the remnant of a much larger primordial population.

Other lines of evidence also favor a much more dense early Kuiper belt. Accretion models show that the objects could not reach their present sizes unless the Kuiper belt originally contained tens of Earth masses of material, whereas its present mass is of order 0.1 $M_{\oplus}$. Accretion occurred as planetesimals collided at low velocities in an environment of low dynamical excitation. In a recent model by Levison and Morbidelli (2003) the zone of formation of Kuiper belt objects is closer to the Sun than their present positions, and they were subsequently pushed outward as Neptune migrated to larger heliocentric distances. This resulted in a dynamical excitation that increased encounter velocities, leading to collisional disruption and mass depletion. Stern and Kenyon (2003) note that the timescale for collisional disruption of bodies of 100 km size is long and that fewer than 1% of them have been catastrophically disrupted. Smaller bodies of order 1 km in radius are catastrophically disrupted by collisions of timescales 100 to 1000 times shorter, with the result that the great majority of the KBOs of the size of ordinary comets are freshly disrupted.

Multi-color photometry and spectroscopic observations have not kept pace with the discoveries of KBOs and Centaurs because of the need for large-aperture telescopes, but color data and spectra for a number of objects in various categories

and dynamical subclasses are emerging. The most extensive on-going compilation of colors of OSS bodies is that of Hainaut and Delsanti (2002). Efforts to obtain photometric data for a large sample of objects are in progress by Noll *et al.* (2002) and others. Jewitt (2002) compiled and analyzed the colors (treated as a spectral gradient in the region ∼0.4-0.7 μm) of a sample of Kuiper belt objects, Centaurs, Trojan asteroids, comet nuclei, and extinct comets, and concluded that extinct comet colors are distinctly different from those of their progenitor Kuiper belt objects and Centaurs.

A few KBOs have been studied spectroscopically, and ice absorption bands at 1.6, 2.0, and 2.3 μm reveals the presence of H_2O ice in some of them. The bands tend to be weak, as is expected for ice mixed with low-albedo minerals or organic solids. Brown *et al.* (1999) found ice bands on 1996 TO_{66}, and Brown (2003) has found ice bands on 50000 Quaoar. See Dotto *et al.* (2003) and Barucci *et al.* (2004) for more complete reviews.

In the absence of signature spectroscopic features (beyond the H_2O ice seen in a few objects) that might lead to the identification of specific minerals, other ices, or other material, we turn to the indirect analytical technique of modeling the color. Color can be expressed in terms of a spectral gradient, or the normalized slope S (% per 100 nm) of the reflectance after correction for the color of the Sun (e.g., Jewitt, 2002). A positive gradient represents a red color, with the continuum intensity increasing toward longer wavelengths.

Continuum gradients in the spectral reflectance also occur at $\lambda \geq 1$ μm, extending to wavelengths at which the reflected sunlight exceeds the thermal emission from a surface. Thermal emission depends on the temperature of a planetary surface, hence its heliocentric distance and albedo. For objects in the outer Solar System where $T \leq 80$ K, thermal emission becomes significant only at $\lambda \geq 10$ μm. For a few of the small bodies in the OSS there are data extending to 2.5 μm, and color is often defined in terms of the standard JHK photometric bands (1.22, 1.65, and 2.18 μm, respectively).

Barucci *et al.* (2001) made a statistical analysis of BVRIJ colors of 15 KBOs and 7 Centaurs and found a continuous spread of colors from neutral to very red. They defined four groups based on two principal components (eigenvectors of the variance-covariance matrix of the colors) that measure the degree of redness; these groups are shown as geometric albedo in Figure 4.

Cruikshank and Dalle Ore (2003) have modelled the colors of KBOs in the Barucci *et al.* groups to constrain or identify materials that lack signature spectral absorption bands, but can be inferred on the basis of spectral slope, primarily in the region $0.3 \leq \lambda \leq 2.5 \mu$m, plus the albedo, a measure of the absolute reflectance. Normalized reflectance is insufficient for modeling a planetary surface, and the additional constraint of the absolute level of reflectance at every wavelength is an important discriminating factor in achieving a model with realistic components. The geometric albedo of a surface is a complex, non-linear function of the composition, grain size, and mixing parameters of the surface components. The albedos

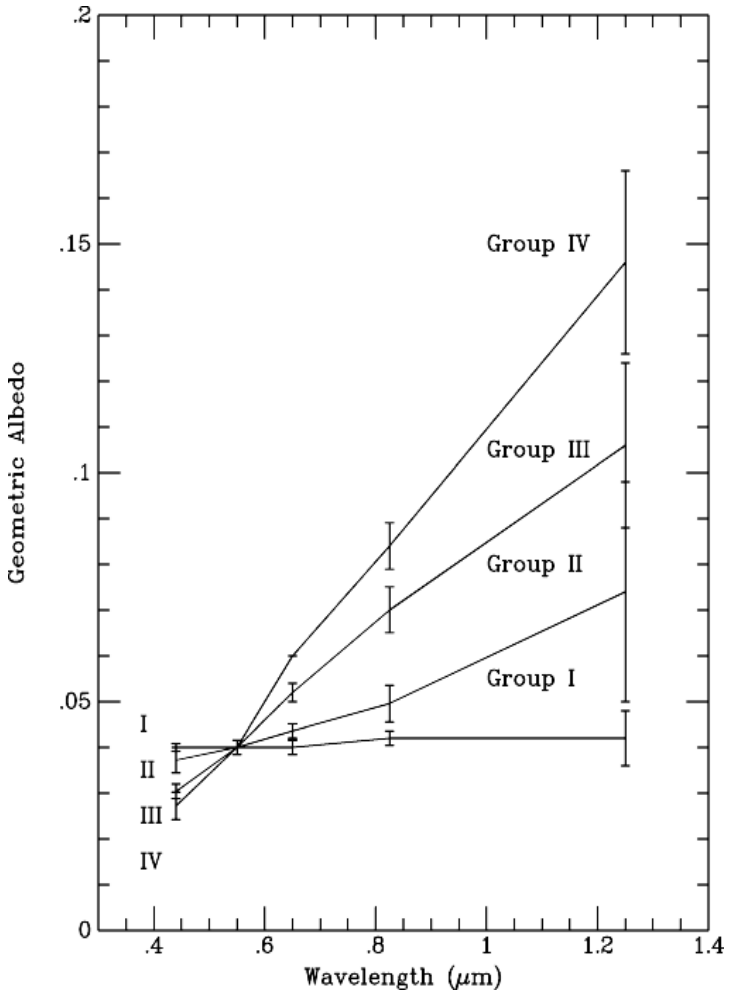

Figure 4. Four groups defined by photometry of Centaurs and Kuiper belt objects by Barucci *et al.* (2001). Representative members of the groups are: Group I (1996 TO_{66}, 2060 Chiron), Group II (10199 Chariklo, 1998 SG35), Group III (1993 SC, 1997 CQ29), Group IV (5145 Pholus, 1994 TB). These curves are normalized to geometric albedo 0.04 at wavelength 0.56 μm.

of Centaurs and Kuiper belt objects are known in only a few cases (e.g., Dotto *et al.*, 2003), and lie in the range 0.04-0.17. Most other OSS objects (small and irregular planetary satellites, Trojan asteroids, and comet nuclei) have albedos in the range 0.02-0.07. Cruikshank and Dalle Ore adopted a geometric albedo of 0.05 at λ = 0.56 μm; the models will pertain also to higher albedo objects with the same spectral slopes, with a reduction in the contribution of the neutral, low-albedo (amorphous carbon) model component.

Cruikshank and Dalle Ore (2003) matched the geometric albedos and colors of the reddest color groupings of outer Solar System bodies with models computed

with scattering theory and the use of optical properties of synthetic organic solids (tholins), particularly Ice Tholin II and Titan tholin. In their models, elemental amorphous carbon was added to the organic solids to achieve the low geometric albedos observed or assumed for these objects. The presence of elemental carbon can occur in nature by the dehydrogenation of tholins. In the use of tholins to achieve the observed red colors, these model results are consistent with those of several other investigators, including the recent work of Dotto *et al.* (2003) and Doressoundiram *et al.* (2003). The least red objects in the outer Solar System can be modeled with mafic minerals, and do not require the presence of organic solids (Cruikshank *et al.*, 2001), while Emery and Brown (2003) showed that certain large classes of organics are specifically excluded by their mafic mineral models of red Trojan asteroids. For additional discussion of quantitative modeling of KBOs and Centaurs see Cruikshank *et al.* (2003).

The Moon, Mercury, and many asteroids are reddened by a space-weathering process consisting of sputtering of iron from iron-bearing minerals, and the deposition of neutral Fe on grains in the uppermost regolith. When space-weathered minerals found on the lunar surface were incorporated into their models, Cruikshank and Dalle Ore (2003) found that the presence of neutral Fe is not required to achieve the observed albedos and colors, although such space-weathered minerals may occur in modest quantities in the optically accessible surfaces.

4.3. OORT CLOUD

In his classic study of the source region of the long-period comets ($P \geq 200$ y) Oort (1950) postulated that about a trillion (10^{12}) icy objects exist in a swarm, or "cloud", centered on the Sun. Each of these objects is in a very large orbit around the Sun, and their periods are longer than about a million years. This swarm is now called the Oort Cloud; its outer extent lies about 1/3 of the way to the next star, or about 100,000 AU (1.5 lightyears) from the Sun. Objects at this great distance are only weakly bound to the Sun, and they are subject to perturbations by the effects of nearby stars and the passage of the Sun and Solar System through a giant molecular cloud in the Galaxy. Such passages occur once every 300-500 million years. In addition, galactic tides (the non-uniform stretching of the Solar System by the gravity field of the center of our Galaxy) can also perturb the orbits of Oort Cloud and cause them to make close passages by the Sun and planets.

Over the course of a million years, about 12 stars pass closely enough to the Solar System to perturb some of the objects in the Oort Cloud. A star is expected to pass within 10,000 AU of the Solar System every 36 million years, and within 3,000 AU every 400 million years, on average. By some estimates, perturbations of the Oort Cloud by such passages can trigger comet showers lasting 2-3 million years, with up to 300 times the normal rate of comets coming in from the Cloud (Weissman, 1998).

The estimated total mass of the icy objects in the Oort Cloud is about 40 $M_\oplus$. The Oort Cloud may be receiving Kuiper belt objects from the scattered disk population. Fernández and Brunini (2000) integrated the orbits of the known scattered disk objects and found that on dynamical half-time of ∼2.5 Gy, about one-third of the objects ended up in the Oort Cloud.

The discovery of a possible member of the inner region of the Oort Cloud (Brown *et al.*, 2004) offers a unique opportunity to study the physical properties of the most distant known object in the Solar System. Brown *et al.* (2004) discovered 2003 VB12 ("Sedna"), which has an inclined (11.9°), highly eccentric (0.84±0.01) orbit with a perihelion distance of 76±4 AU and a semimajor axis of 480±40 AU. Sedna appears to be rotating very slowly (P≥20 days), suggesting the presence of a (so far) unseen satellite. Sedna's thermal flux has remained undetected, suggesting a diameter of ∼1800 km or a bit less. The color of Sedna is very red, comparable to 5145 Pholus (see above), although the spectral features exhibited by Pholus have not yet been detected.

The orbital characteristics have suggested at least three scenarios of origin. Sedna may have been scattered into its present orbit by an unseen planet with mass ∼1 $M_\oplus$ at a heliocentric distance of ∼70 AU; Brown *et al.* (2004) note that none of the known planets in the Solar System can dynamically excite objects from the inner Oort Cloud. Another possibility is that an encounter by a high velocity passing star perturbed Sedna out of the Oort Cloud and into its present orbit. A third scenario, regarded as more likely by Brown *et al.* (2004), has the Sun forming in a star cluster where low-velocity encounters with neighboring stars were frequent. All three possibilities predict the existence of several other objects in orbits comparable to that of Sedna.

Continuing surveys in the trans-Neptunian region, including those anticipated employing powerful new techniques, will produce many new, intriguing, and challenging discoveries. We can hope and expect that such discoveries will further elucidate and clarify the emerging picture of the origin and evolution of the Solar System and the growing number of recognized extrasolar planetary systems.

References

Andronico, G., Baratta, G.A., Spinella, F., and Strazzulla, G.: 1987, 'Optical evolution of laboratory-produced organics – applications to Phoebe, Iapetus, outer belt asteroids and cometary nuclei', *Astron. Astrophys.* **184**, 333–336.

Barucci, M.A., Fulchignoni, M., Birlan, M., Doressoundiram, A., Romon, J., and Boehnhardt, H.: 2001, 'Analysis of Trans-Neptunian and Centaur colours: continuous trend or grouping?', *Astron. Astrophys.* **371**, 1150–1154.

Barucci, M.A., Doressoundiram, A., and Cruikshank, D.P.: 2004, in M.C. Festou, H.U. Keller, and H.A. Weaver (eds.), *Comets II*, The University of Arizona Press, in press.

Binzel, R.P. and Hubbard, W.B.: 1997, 'Mutual events and stellar occultations', in S.A. Stern and D.J. Tholen (eds.), in *Pluto and Charon*, The University of Arizona Press, Tucson, pp. 85-102.

Bockelée-Morvan, D., Lellouch, E., Biver, N., Paubert, G., Bauer, J., Colom, P., and Lis, D.C.: 2001, 'Search for CO gas in Pluto, Centaurs and Kuiper belt objects at radio wavelengths', *Astron. Astrophys.* **377**, 343–353.

Broadfoot, A.L., *et al.*: 1989, 'Ultraviolet spectrometer observations of Neptune and Triton', *Science* **246**, 1459–1466.

Brown, M.E.: 2003, *Bull. Am. Astron. Soc.* **35**, 969 (abstract).

Brown, M.E. and Calvin, W.M.: 2000, 'Evidence for crystalline water and ammonia ices on Pluto's satellite Charon', *Science* **287**, 107–109.

Brown, M.E., Trujillo, C., and Rabinowitz, D.: 2004, *Astrophys. J. Lett.*, in press.

Brown, R.H. and Cruikshank, D.P.: 1993, 'Remote sensing of ices and ice-mineral mixtures in the outer solar system', in C.M. Pieters, and P.A.J. Englert (eds.), *Remote Geochemical Analysis: Elemental and Mineralogical Composition*, The Cambridge University Press, pp. 455–468.

Brown, R.H., Cruikshank, D.P., Veverka, J., Helfenstein, P., and Eluszkiewicz, J.: 1995, 'Surface composition and photometric properties of Triton', in D.P. Cruikshank (ed.), *Neptune and Triton*, The University of Arizona Press, Tucson, pp. 991–1030.

Brown, R.H., Cruikshank, D.P., Pendleton, Y.J., and Veeder G.J.: 1998, 'Identification of water ice on the Centaur 1997 CU26', *Science* **280**, 1430–1432.

Brown, R.H., Cruikshank, D.P., and Pendleton, Y.J.: 1999, 'Water ice on Kuiper belt object 1996 TO_{66}', *Astrophys. J.* **519**, L101–L104.

Calcagno, L., Foti, G., Torrisi, L., and Strazzulla, G.: 1985, 'Fluffy layers obtained by ion bombardment of frozen methane Experiments and applications to Saturnian and Uranian satellites', *Icarus* **63**, 31–38.

Cruikshank, D.P.: 1987, 'Dark matter in the solar system', *Adv. Space Res.* **7**, 109–120.

Cruikshank, D.P. (ed.): 1995, *Neptune and Triton*, The University of Arizona Press, Tucson, 1249 pp.

Cruikshank, D.P. and Dalle Ore, C.M.: 2003, 'Spectral models of Kuiper belt objects and Centaurs', *Earth, Moon, and Planets* **92**, 315–330.

Cruikshank, D. P., Roush, T. L., Owen, T. C., Quirico, E., and de Bergh, C.: 1998a, 'The surface compositions of Triton, Pluto and Charon', in B. Schmitt, C. de Bergh, and M. Festou (eds.), *Ices in the Solar System*, Kluwer Academic Publishers, Dordrecht, pp. 655–684.

Cruikshank, D.P., *et al.*: 1998b, 'The composition of Centaur 5145 Pholus', *Icarus* **135**, 389–407.

Cruikshank, D.P., *et al.*: 1998c, *Bull. Am. Astron. Soc.* **30**, 1094 (abstract).

Cruikshank, D.P., Dalle Ore, C.M., Roush, T.L., Geballe, T.R., Owen, T.C., de Bergh, C., Cash, M.D., and Hartmann, W.K.: 2001, *Icarus* **153**, 348–360.

Cruikshank, D.P., Roush, T.L., and Poulet, F.: 2003, 'Quantitative modeling of the spectral reflectance of Kuiper belt objects and Centaurs', *C. R. Physique* **4**, 783–789.

Cruikshank, D.P., Dalle Ore, C.M., and Imanaka, H.: 2005, *Icarus*, submitted.

Davies, J.K., Sykes, M.V., and Cruikshank, D.P.: 1993, 'Near-infrared photometry and spectroscopy of the unusual minor planet 5145 Pholus (1992AD)', *Icarus* **102**, 166–169.

Doressoundiram, A., Tozzi, G.P., Barucci, M.A., Boehnhardt, H., Fornasier, S., and Romon, J.: 2003, 'ESO Large Programme on Trans-Neptunian Objects and Centaurs: Spectroscopic Investigation of Centaur 2001 BL41 and TNOs (26181) 1996 GQ21 and (26375) 1999 DE9', *Astron. J.* **125**, 2721–2727.

Dotto, E., Barucci, M. A., and de Bergh, C.: 2003, *C. R. Physique* **4**, 775–782.

Douté, S., Schmitt, B., Quirico, E., Owen, T.C., Cruikshank, D.P., de Bergh, C., Geballe, T.R., and Roush, T.L.: 1999, 'Evidence for methane segregation at the surface of Pluto', *Icarus* **142**, 421–444.

Dumas, C., Terrile, R.J., Brown, R.H., Schneider, G., and Smith, B.A.: 2001, 'Hubble Space Telescope NICMOS spectroscopy of Charon's leading and trailing hemispheres', *Astron. J.* **121**, 1163–1170.

Elliot, J.L., Dunham, E.W., Bosh, A.S., Silvan, S.M., Young, L.A., Wasserman, L.H., and Millis, R.L.: 1989, *Icarus* **77**, 148–170.

Elliot, J.L. and Young, L.A.: 1992, *Astron. J.* **103**, 991–1015.
Elliot, J.L., *et al.*: 1998, 'Global warming on Triton', *Nature* **393**, 765–767.
Elliot, J.L., *et al.*: 2003, 'The recent expansion of Pluto's atmosphere', *Nature* **424**, 164–168.
Emery, J.P. and Brown, R.H.: 2003, 'Constraints on the surface composition of Trojan asteroids from near-infrared (0.8-4.0 μm) spectroscopy', *Icarus* **164**, 104–121.
Fernández, J.A. and Brunini, A.: 2000, *Icarus* **145**, 580–590.
Funato, U., Makino, J., Hut, P., Kokubo, E., and Kinoshita, D.: 2004, 'The formation of Kuiper-belt binaries through exchange reactions', *Nature* **427**, 518–520.
Gaffey, S.J., McFadden, L.A., Nash, D., and Pieters, C.M.: 1993, 'Ultraviolet, visible, and near-infrared reflectance spectroscopy: laboratory spectra of geologic materials', in C.M. Pieters and P.A.J. Englert (eds.), *Remote Geochemical Analysis: Elemental and Mineralogical Composition*, Cambridge University Press, New York, pp. 43–77.
Goldreich, P., Lithwick, Y., and Sari, R.: 2002, 'Formation of Kuiper-belt binaries by dynamical friction and three-body encounters', *Nature* **420**, 643–646.
Grundy, W.M., Buie, M.W., and Spencer, J.R.: 2002, 'Spectroscopy of Pluto and Triton at 3–4 microns: possible evidence for wide distribution of nonvolatile solids', *Astron. J.* **124**, 2273–2278.
Hainaut, O.R. and Delsanti, A.C.: 2002, 'Colors of minor bodies in the Outer solar system. A statistical analysis', *Astron. Astrophys.* **389**, 641–664.
Hartmann, W.K., Tholen, D.J., and Cruikshank, D.P.: 1987, 'The relationship of active comets, 'extinct' comets, and dark asteroids', *Icarus* **69**, 33–50.
Hartmann, W.K., Tholen, D.J., Meech, K.J., and Cruikshank, D.P.: 1990, '2060 Chiron – colorimetry and cometary behavior', *Icarus* **83**, 1–15.
Jewett, D.C.: 'From Kuiper belt object to cometary nucleus: The missing ultrared matter', *Astron. J.* **123**, 1039–1049.
Jewitt, D. and Luu, J.: 1993, 'Discovery of the candidate Kuiper belt object 1992 QB1', *Nature* **362**, 730–732.
Khare, B.N., Sagan, C., Arakawa, E.T., Suits, R., Callcot, T.A., and Williams, M.W.: 1984, 'Optical constants of organic tholins produced in a simulated Titanian atmosphere - From soft X-ray to microwave frequencies', *Icarus* **60**, 127–137.
Khare, B.N., Thompson, W. R., Cheng, L., Chyba, C., Sagan, C., Arakawa, E. T., Meisse, C., and Tuminello, P.: 1993, 'Production and optical constraints of ice tholin from charged particle irradiation of (1:6) C_2H_6/H_2O at 77 K', *Icarus* **103**, 290–300, 1993.
Krasnopolsky, V.A. and Cruikshank, D.P.: 1995, 'Photochemistry of Triton's atmosphere and ionosphere', *J. Geohys. Res.* **100**, 21,271–21,286.
Krasnopolsky, V.A. and Cruikshank, D.P.: 1999, 'Photochemistry of Pluto's atmosphere and ionosphere near perihelion', *J. Geophys. Res.* **104**, 21,979–21,996.
Kuiper, G.P.: 1951, 'On the origin of the solar system', in J.A. Hynek (ed.), *Astrophysics*, New York: McGraw-Hill, New York, pp. 357–424.
Lellouch, E., Laureijs, R., Schmitt, B., Quirico, E., de Bergh, C., Crovisier, J., and Coustenis, A.: 2000, 'Pluto's non-isothermal surface', *Icarus* **147**, 220–250.
Levison, H.F. and Morbidelli, A.: 2003, 'The formation of the Kuiper belt by the outward transport of bodies during Neptune's migration', *Nature* **426**, 419–421.
Luu, J., Jewitt, D., and Cloutis, E.: 1994, *Icarus* **109**, 133–144.
McKinnon, W.B., Lunine, J.I., and Banfield, D.: 1995, 'Origin and evolution of Triton', in D.P. Cruikshank (ed.), *Neptune and Triton* , The University of Arizona Press, Tucson, pp. 807–877.
Miner, E.D. and Wessen, R.R.: 2002, *Neptune: The Planet, Rings and Satellites*, Springer Praxis, Chichester, 297 pp.
Noll, K.S.: 2004, *Earth, Moon, and Planets* **92**, 395–407.
Noll, K., Stephens, D., Grundy, W., Millis, R., Buie, M., Spencer, J., Tegler, S., Romanishin, W., and Cruikshank, D.: 2002, *Bull. Am. Astron. Soc.* **34**, 849 (abstract).

Oort, J.: 1950, 'The structure of the cloud of comets surrounding the solar system and a hypothesis concerning its origin', *Bull. Astron. Inst. Neth.* **11**, 91–110.

Owen, T.C., Cruikshank, D.P., Roush, T., de Bergh, C., Brown, R. H., Bartholomew, M. J., Elliot, J., and Young, L. 1993, 'Surface ices and the atmospheric composition of Pluto', *Science* **261**, 745–748.

Poulet, F., Cuzzi, J.N., Cruikshank, D.P., Roush, T., and Dalle Ore, C.M.: 2002, 'Comparison between the Shkuratov and Hapke scattering theories for solid planetary surfaces: Application to the surface composition of two Centaurs', *Icarus* **160**, 313–324.

Quirico, E., Douté, S., Schmitt, B., de Bergh, C., Cruikshank, D.P., Owen, T.C., Geballe, T.R., and Roush, T.L.: 1999, 'Composition, physical state, and distribution of ices at the surface of Triton', *Icarus* **139**, 159–178.

Sicardy, B., *et al.*: 2003, 'Large changes in Pluto's atmosphere as revealed by recent stellar occultations', *Nature* **424**, 168–170.

Stansberry, J.A., Lunine, J.I., Hubbard, W.B., Yelle, R.V., and Hunten, D.M.: 1994, 'Mirages and the nature of Pluto's atmosphere', *Icarus* **111**, 503–513.

Stern, S.A., Buie, M.W., and Trafton, L.: 1997, 'HST high-resolution images and maps of Pluto', *Astron. J.* **113**, 827–843.

Stern, S.A. and Kenyon, S.J.: 2003, 'Collisions, accretion, and erosion in the Kuiper belt', *C. R. Physique* **4**, 803–808.

Stone, E.C. and Miner, E.D: 1989, 'The Voyager 2 encounter with the Neptunian system', *Science* **146**, 1417–1421.

Strobel, D.F., Zhu, X., Summers, M.E., and Stevens, M.H.: 1996, 'On the vertical thermal structure of Pluto's atmosphere', *Icarus* **120**, 266–289.

Tholen, D.J. and Buie, M.W.: 1997, 'The Orbit of Charon', in S.A. Stern and D.J. Tholen (eds.), *Pluto and Charon*, The University of Arizona Press, Tucson, pp. 193–219.

Tyler, G.L., Sweetnam, D.N., Anderson, J.D., Borutzki, S.E., Campbell, J.K., Kursinski, E.R., Levy, G.S., Lindal, G.F., Lyons, J.R., and Wood, G.E.: 1989, 'Voyager radio science observations of Neptune and Triton', *Science* **246**, 1466–1473.

Weidenschilling, S.J.: 2002, 'On the origin of binary transneptunian objects', *Icarus* **160**, 212–215.

Weissman, P.R.: 1998, 'The Oort cloud', *Scientific American* **279**, 84–89.

Yelle, R.V., Lunine, J.L., and Hunten, D.M.: 1991, 'Energy balance and plume dynamics in Triton's lower atmosphere', *Icarus* **89**, 347–358.

Young, L.A., Elliot, J.L., Tokunaga, A., de Bergh, C., and Owen, T.: 1997, 'Detection of gaseous methane on Pluto', *Icarus* **127**, 258–262.

Young, E.F., Binzel, R.P., and Crane, K.: 2001, 'A two-color map of Pluto's sub-Charon hemisphere', *Astron. J.* **121**, 552–561.

Address for Offprints: Dale P. Cruikshank, Astrophysics Branch (Mail Stop 245-6), NASA Ames Research Center, Moffett Field, CA 94035-1000, USA; Dale.P.Cruikshank@nasa.gov